BJ www.biochemj.org

BJ Structure

Biochem. J. (2009) **424**, 335–345 (Printed in Great Britain) doi:10.1042/BJ20090825

online data

SUPPLEMENTARY ONLINE DATA

A constitutively active and uninhibitable caspase-3 zymogen efficiently induces apoptosis

Jad WALTERS*, Cristina POP†, Fiona L. SCOTT†, Marcin DRAG†[1], Paul SWARTZ*, Carla MATTOS*, Guy S. SALVESEN† and A. Clay CLARK*[2]

*Department of Molecular and Structural Biochemistry, North Carolina State University, Raleigh, NC 27695, U.S.A., and †Program in Apoptosis and Cell Death, The Burnham Institute for Medical Research, 10901 N Torrey Pines Rd, La Jolla, CA 92037, U.S.A.

The interface mutants do not affect oligomerization

Although the V266E mutation does not change the oligomeric properties of caspase-3 at higher protein concentrations (micromolar range) [1], we examined whether the mutation weakens the dimer interface at lower protein concentrations by performing dilution experiments coupled with enzyme activity measurements (see Figure S1). The data follow a unimolecular mechanism, suggesting that, at least in the presence of the substrate, the caspase-3 mutants were stable dimers in the picomolar range of protein concentration.

The interface mutants kill cells independently of endogenous caspase-3

Because the substrate specificity is the same for the V266E variants and WT (see Figure 1D in the main text), it is likely that the mutants cleave the same substrates as caspase-3 during apoptosis. Alternatively, it is possible that the interface mutants activate the endogenous caspase-3, which then amplifies the downstream proteolytic events, although this is unlikely given that procaspase-3 is typically a poor substrate for active caspase-3 [2]. To examine the latter possibility, we transfected MCF7 cells, which lack endogenous caspase-3 [3], with plasmids containing the interface mutants, and we measured apoptosis by Annexin V staining (see Figure S4A). Although the transfection efficiency was lower than in the case of HEK-293A cells ($\sim 35\,\%$ compared with $\sim 60\,\%$ respectively), the pattern of cell death observed in the HEK-293A cells (see Figure 2A in the main text) was reproduced in the MCF7 cells (see Figure S4A). One should note that Bax, the positive control, was less toxic in MCF7 cells than were the interface mutants due to the lack of endogenous caspase-3, the main effector caspase. In all cases, the number of apoptotic cells diminished in the presence of the caspase inhibitor Z-VAD-FMK.

Similarly, recombinant V266E cleaved caspase substrates in the absence of caspase-3 when added to crude cellular extracts. We examined hypotonic lysates from Jurkat cells that were immunodepleted of the endogenous caspase-3 and reconstituted with recombinant caspase-3 proteins. The lysates were analysed by Western blot for cleavage of ICAD (see Figure S4B). We observed that ICAD was cleaved efficiently by the active WT and V266E proteins, and it remained unprocessed upon addition of the less active procaspase-3. The cleavage of ICAD was judged by the disappearance of the full-length protein for which the antibodies were developed. Lysate prepared from cells treated with Z-VAD-FMK showed no DEVD-ase activity (results not shown).

Conserved water molecules in the dimer interface

On one side of the interface, α-helices 5 and 5′ border β-strands 8 and 8′, whereas the opposite face has a water-filled cavity (see [4] for review). Moreover, several of the water molecules found in the central cavity are conserved. We examined over 5000 crystallographic water molecules in 20 caspase-3 structures with a resolution of 2.5 Å or better, including proteins from our own studies as well as those deposited in the PDB. We considered water molecules that were within 1.4 Å of one another to be conserved, using a previously published method [4a]. The structures included in our conserved water analysis were obtained from crystals with symmetry of various space groups formed under different crystallization conditions and differing in the number of molecules per asymmetric unit. Overall, the analysis identified several conserved water molecules throughout the structure of caspase-3, but we focus in the present study on six conserved hydration sites in the dimer interface, which are found in a pseudo-planar arrangement approx. 3.8 Å above the $Val^{266}/Val^{266'}$ side chains (see Figure 4B of the main text).

In WT, Wat219 (where Wat is a water molecule) and Wat219′ H-bond with the hydroxy groups of Tyr^{197} and $Tyr^{197'}$ respectively. Both of these water molecules also interact with four central crystallographic water molecules to provide a H-bonding network bridging the two active sites. Wat192 and Wat192′ in this network also H-bond to Arg^{164} and $Arg^{164'}$ respectively. The water network is disrupted in V266E, where Wat219 and Wat219′ are removed, and the four central water molecules move to prevent clashes with Glu^{266} (Figure 4B). Interestingly, the carboxylates of Glu^{266} and $Glu^{266'}$ displace Wat108 and Wat108′ respectively, and maintain the planar contacts with Wat192 and Wat192′. Overall, this arrangement preserves the H-bonding network between Arg^{164} and $Arg^{164'}$, but removes H-bonds contributed by Tyr^{197} and $Tyr^{197'}$.

EXPERIMENTAL

Positional scanning libraries

In the first step, Fmoc (fluoroen-9-ylmethoxycarbonyl)-ACC fluorophore was coupled to the Rink Amide Resin (Novabiochem) using a procedure described previously [5]. The Fmoc protecting group was removed using 20 % piperidine in DMF (dimethylformamide). Coupling of the Fmoc-Asp(O-tBut)-COOH was carried out in DMF using HATU as the coupling reagent and in the presence of the 2,4,6-collidine base for 24 h at room temperature. This step was repeated twice. The unreacted ACC was acetylated as described previously [5]. The Fmoc protecting

[1] Current address: Division of Medicinal Chemistry and Microbiology, Faculty of Chemistry, Wroclaw University of Technology, Wybrzeze Wyspianskiego 27, 50-370 Wroclaw, Poland

[2] To whom correspondence should be addressed (email clay_clark@ncsu.edu).

The atomic co-ordinates and structure factors for caspase-3(V266E) have been deposited in the PDB under accession code 3ITN.

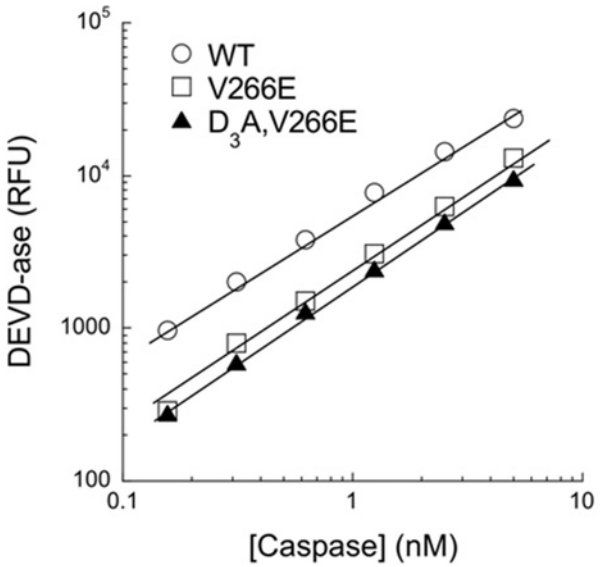

Figure S1 Dilution studies of the V266E interface mutants

The indicated caspase-3 proteins were diluted in standard assay buffer at concentrations between 0.15 and 10 nM and incubated for 15 min at 37 °C. The enzymatic activity was determined against 100 μM Ac-DEVD-AFC.

group was removed using 20 % piperidine in DMF and, after washing with DMF, dichloromethane, THF (tetrahydrofolate) and methanol, the resin was dried in vacuum. The resin was distributed in 75 mg portions into 57 wells of a 96-deep-well plate (semi-automatic FlexChem synthesizer). Standard peptide synthesis was used to prepare the libraries. The amino acid or mixture of amino acids, HOBt and DICI were preincubated for 4 min and added to the appropriate wells and agitated for 3 h along with 30 min Fmoc decouplings in 20 % piperidine in DMF. The variable amino acid mixtures were prepared as an isokinetic mixture with 19 amino acids (all amino acids omitting cysteine and methionine due to the oxidation problems; norleucine was used to mimic methionine). The N-termini of the tetrapeptides were capped with acetate (Ac_2O and DIEA in DMF) for 2 h. The resin was washed with DMF, dichloromethane, THF and methanol, and the resin was dried in vacuum for 24 h. The cleavage of the substrates was carried out for 1.5 h at room temperature using the mixture of 92.5 % TFA (trifluoroacetic acid), 2.5 % water, 2.5 % tri-isopropyl silane and 2.5 % phenol (1.5 ml per well). After cleavage, TFA was removed and the substrates were precipitated for 10 min at 0 °C using t-butyl-methyl ether (12 ml) and centrifuged. This step was repeated once. Subsequently, all ACC substrates were dissolved in water/dioxane (1:1, v/v) and freeze-dried for 48 h. Finally, all individual substrates were dissolved as stock solutions at concentration of 50 mM in biological purity DMSO and stored frozen.

RT–PCR

HEK-293A cells, transfected with caspase-3 mutants and in the presence of 100 μM ZVAD-FMK, were harvested and lysed in TRizol® reagent (Invitrogen). The total RNA was extracted using TRizol® as recommended by the manufacturer's instructions and resuspended in 50 μl of DEPC-treated water. Contaminating genomic/plasmidial DNA was removed from the total RNA solution by using the DNase free kit (Ambion). To prepare the first strand cDNA, ~1 μg of (DNA-free) RNA was primed with oligo(dT) and subjected to RT in 20 μl final volume by using the SuperScriptIII kit from Invitrogen. Control reactions did not include the reverse transcriptase enzyme in the reaction mixture. All cDNA samples (~200 ng) were amplified by PCR using either caspase-3-specific primers (forward: caspase-3 internal primer; reverse: FLAG-tag primer) or primers designed to amplify a housekeeping gene such as α-tubulin. Samples were run in 0.8 % agarose gel and stained with ethidium bromide. The DNA molecular ladder was from Invitrogen (DNA 1 kb plus).

Cell lysate preparation

HEK-293A or MCF7 cells were harvested as described above, washed with PBS, and the cell pellet was frozen at −20°C for a maximum of 3 days. Thawed cell pellets were lysed on ice for 10 min with mRIPA buffer [modified radioimmunoprecipitation buffer; 10 mM Tris/HCl, pH 7.4, 150 mM NaCl, 1 % (v/v) Nonidet P40, 0.5 % deoxycholate,

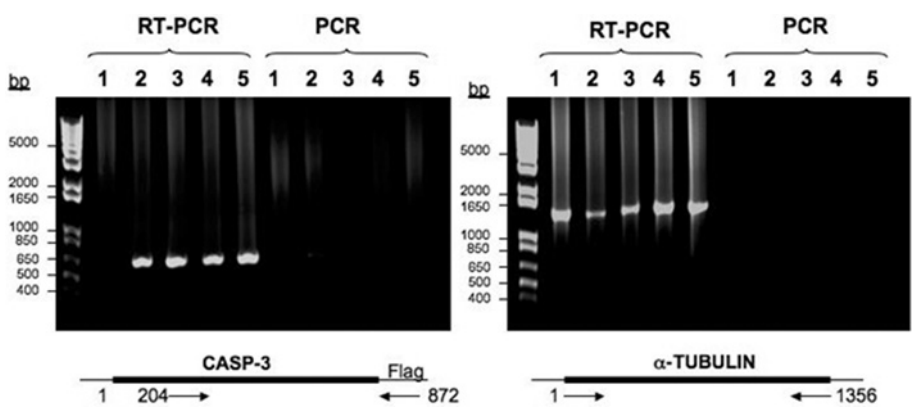

Figure S2 RT–PCR reactions of DNA-free RNA isolated from transfected HEK-293A cells

The following FLAG-tagged constructs were used: 1, vector control; 2, caspase-3 (WT); 3, procaspase-3(D_3A); 4, caspase-3(V266E); 5, procaspase-3(D_3A,V266E). The PCR reactions used specific primers for caspase-3–FLAG and α-tubulin, depicted at the bottom of each panel. To rule out the possibility of plasmidial/genomic DNA contamination, control reactions (PCR) used RNA samples subjected to RT reactions in the absence of the reverse transcriptase.

0.1 % SDS and 5 mM EDTA] containing the following protease inhibitors: 50 μM DCI (dichloroisocoumain), 50 μM leupeptin, 50 μM MG132 and 10 μM E-64. Lysates were clarified by centrifugation at 15 000 ***g*** for 15 min. For preparation of hypotonic Jurkat lysates, cells were treated as described previously [6]. Jurkat lysates were immunodepleted for caspase-3 by incubation with caspase-3 antibodies diluted 1:100 (BD clone 19) overnight at 4 °C, followed by the addition of Protein A/G beads for 2 h [7]. Depleted Jurkat cell lysates were reconstituted with recombinant caspase-3 mutants (25 nM final concentration) and incubated at 37 °C to allow caspase substrate processing. The lysates were balanced for protein content before immunoblotting.

Caspase assays

The protein concentrations in the cell lysates were determined using the Bio-Rad DC protein assay, and the lysates were normalized for protein content. To determine the activity of the executioner caspases, cell lysates were diluted 1:5 in caspase assay buffer [10 mM Pipes, pH 7.4, 150 mM NaCl, 0.1 % CHAPS, 10 % (w/v) sucrose and 10 mM DTT], incubated for 15 min at 37°C, and then the rate of hydrolysis of fluorogenic substrate (Ac-DEVD-AFC, 100 μM) was measured. For inhibition studies using XIAP, the recombinant caspase-3 proteins (300–600 pM) were incubated for 30 min at 37 °C in modified caspase buffer [50 mM Hepes, pH 7.4, 100 mM NaCl, 10 % (w/v) sucrose, 0.1 % CHAPS, 20 mM 2-mercaptoethanol] with serial dilutions of XIAP (0–700 nM). Residual activity was determined by the rate of hydrolysis of Ac-DEVD-AFC (100 μM) with an f_{MAX} Fluorescence Plate Reader (Molecular Devices). The apparent inhibition constant $K_{i,app}$ or the IC_{50} was determined from the uninhibited rate (v_o) and inhibited rates (v_i), by plotting the percentage of inhibition ($100 \times v_i/v_0$) against inhibitor concentration [I] as shown in eqn 1:

$$100 \times \frac{v_i}{v_0} = b + \frac{(100 - b) \times K_{i,app}}{K_{i,app} + [I]} \quad (1)$$

where b is the baseline of inhibition at infinite inhibitor concentration. The value for baseline b approaches zero for strict competitive inhibition and is more than 5–10 for mixed

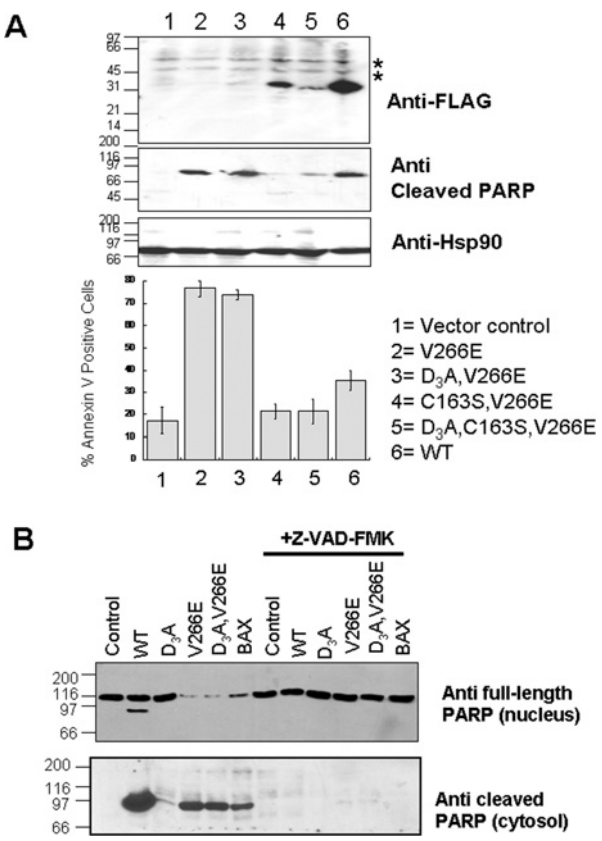

Figure S3 Inactive V266E variants no longer support apoptosis

(**A**) Western blots (upper panels) of cellular lysates from cells transfected with inactive variants of V266E mutants (lower panel). Protein expression and activation was assessed by antibodies against the FLAG tag, for detection of the transfected constructs, or cleaved PARP. Hsp90 panel represents a loading control; *non-specific protein. (**B**) Western blots of the cellular lysates from Figure 2(A) against anti-full-length PARP (nuclear extract) or cleaved PARP (cytosolic extract).

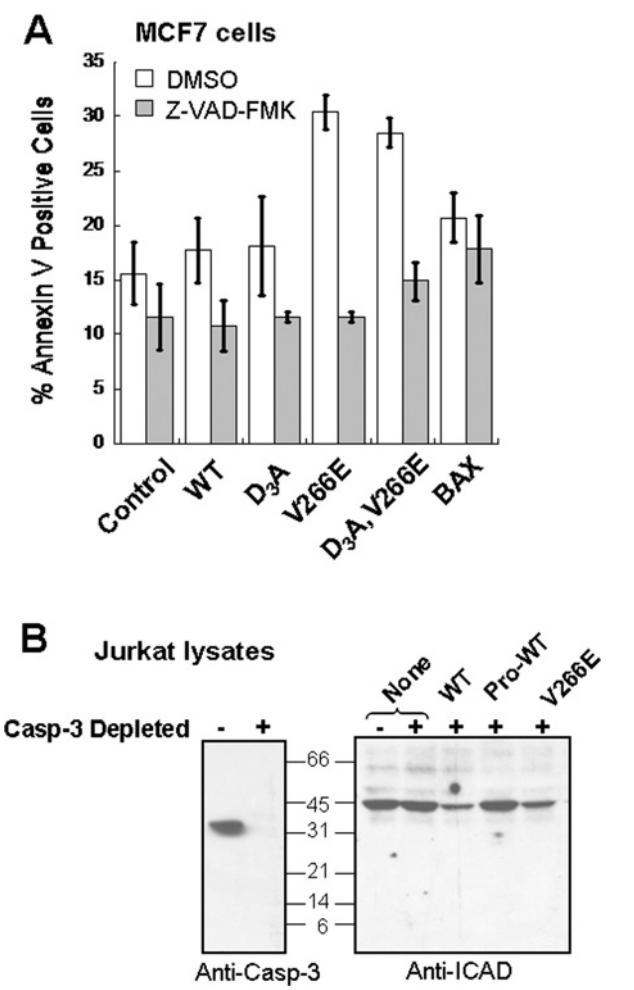

Figure S4 Caspase-3 V266E mutants kill cells independently of the presence of endogenous caspase-3

(**A**) MCF7 cells, which lack procaspase-3, were transfected with 1 μg of total DNA, as described in the legend for Figure 2 of the main text, and 24 h later the cells were quantified by FACS for Annexin V-positive cells. The values represent the means $\pm$ S.D. for three independent experiments. (**B**) Hypotonic Jurkat lysates were immuno-depleted of endogenous caspase-3 (Casp-3 Depleted) and reconstituted with recombinant caspase-3. After incubation at 37 °C, cleavage of ICAD was detected by immunobloting for full-length ICAD.

inhibition. From the Michaelis–Menten constant, K_M, of each caspase mutant for the substrate Ac-DEVD-AFC and substrate concentration [S], the true K_i of inhibition was calculated using eqn 2:

$$K_i = \frac{K_{i,app}}{1 + \frac{S}{K_M}} \quad (2)$$

For inhibition studies using p35, the experiments were carried out as above, except that the concentration of caspase-3 was 2 nM and that of p35 varied between 0 and 12 nM.

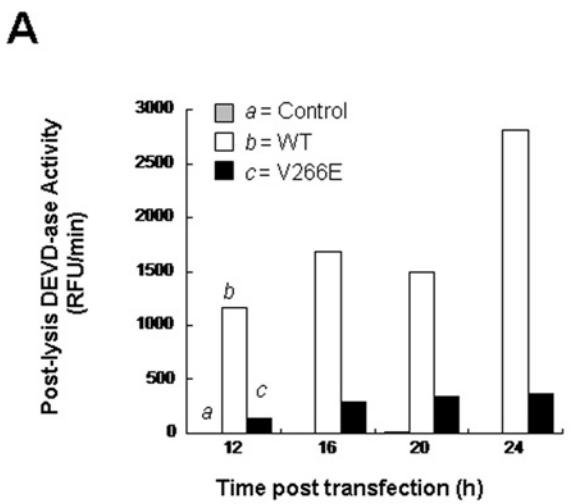

Figure S5 Relative DEVD-ase activity

(**A**) DEVD-ase activity in lysates prepared from cells transfected with WT or V266E for the indicated time periods. (**B**) DEVD-ase activity in culture medium from cells transfected with caspase-3 mutants. Cultures grown in complete growth medium were centrifuged at 500 ***g*** to remove the cells. Supernatant (25 μl) was mixed with 2× assay buffer (25 μl), incubated at 37 °C for 10 min, and the DEVD-ase activity was measured as described in the Experimental section. The activity was normalized to the volume of the cell culture (~ 2.5 ml), but not to the amount of protein from the cell lysates (see Figure 3 of the main text). The y-axis values for DEVD-ase activities generated by cell medium and the cell lysates (see Figure 3 of the main text) are not comparable. RFU, relative fluorescence units.

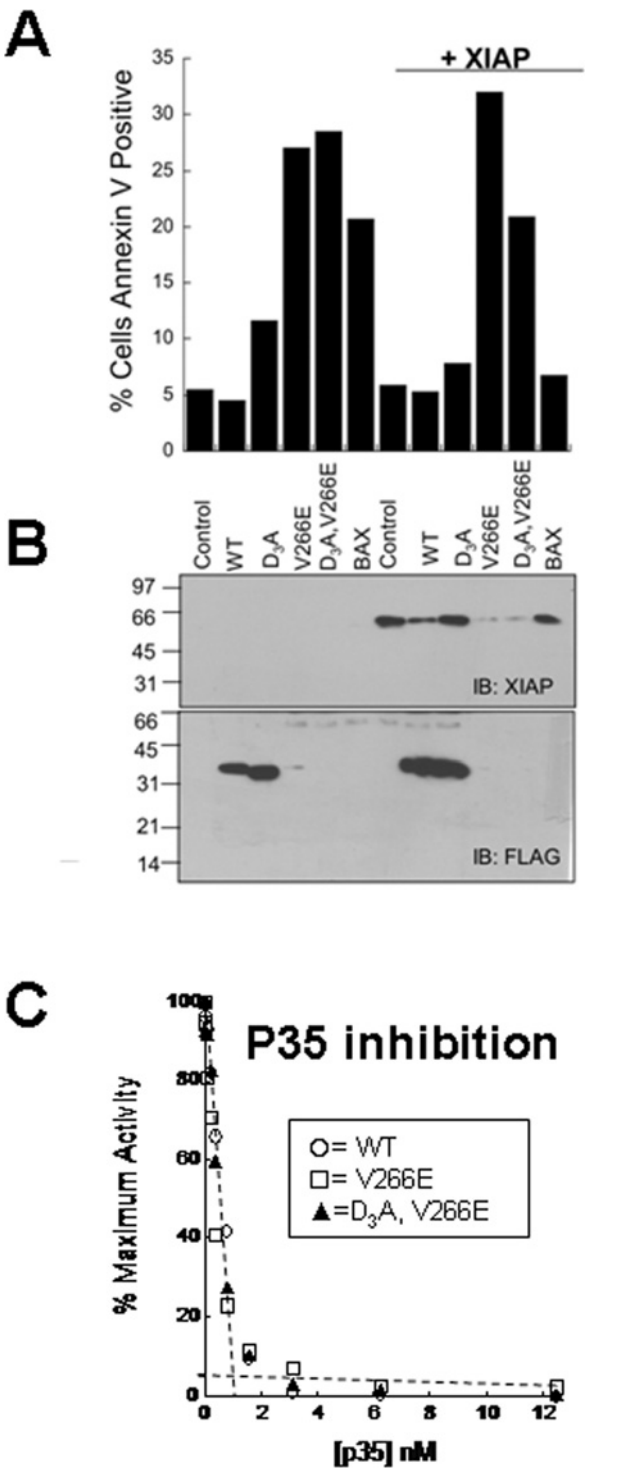

Figure S6 Co-expression of XIAP with the caspase-3 V266E mutants cannot rescue cells from apoptosis

(**A**) HEK-293A cells were transfected with 2 μg of total DNA (1 μg of caspase DNA plus 1 μg XIAP DNA for co-transfections) and, after 24 h, the cells were quantified for Annexin V staining. We note that the values for V266E and D_3A,V266E in the presence of XIAP are not significantly different given the error limits for this experiment. (**B**) Western blot analysis of the samples from (**A**) shows that XIAP does not accumulate in cells containing the caspase-3 V266E mutants. (**C**) All caspase-3 mutants (2 nM) were efficiently titrated with the viral inhibitor p35 at concentrations as low as those approaching the $K_{i,app}$ for inhibition.

Procaspase-3 homology models, energy minimization and molecular dynamics

Models of both the inactive and active procaspase-3 proteins were built as described below, and the program CHARMm version 27 [8] was used for molecular dynamics simulations and energy minimizations to assure that the final models represent energetically feasible structures.

The inactive procaspase-3 model was generated using the alignment mode of the SWISS-MODEL protein structure homology modelling server [9]. The target sequence, procaspase-3, was modelled using procaspase-7 (PDB code 1K88) as the template sequence. ϕ and ψ angles were corrected manually with COOT [10] so that all dihedral angles throughout the entire structure were within accepted values in the Ramachandran plot (see Table S1). The IL in molecule B of procaspase-7 is mostly, but not completely, ordered, such that residues 167–177 (procaspase-3 numbering) are not visible in the electron density maps. It was therefore necessary to build the missing residues in order to obtain the structure of the complete IL. Given the degrees of freedom available for the missing residues in the linker, we acknowledge that our initial model included one of several possible conformations for the missing section. The starting conformation is one in which each additional residue was built to have Φ and ψ angles in optimal regions in the Ramachandran plot, as monitored by the appropriate function in the program COOT, although at the same time connecting the two ends of the IL already present in the model.

The model of active procaspase-3(V266E) was built with the wild-type caspase-3 structure as the template (PDB code 2J30). This is appropriate due to the high levels of activity of D_3A,V266E. On the basis of our previous results [11], Asp^{169} and Val^{189} were used as anchor points, and the IL was built manually using COOT. ϕ and ψ angles were inspected manually during the initial building of the IL, as was performed for the model of the inactive protein. In this case, however, the side chains for the built residues have substantial degrees of freedom and were given common rotamers. The backbone was built over the interface in order to connect the two ends of the IL in a way to form the loop bundle of both active sites, as is observed in active caspase-3.

After the initial building of the two models, any strains or unfavourable conformations were relieved using the CHARMm potential energy function with the PARAM19 parameter set for extended atom representation and an atom-based force switching function applied to non-bonded interactions, with the switch starting at 5 Å and ending at 6 Å. All energy minimizations were performed using a gradient tolerance cutoff of 0.0001.

The initial models were placed in equilibrated 62 Å cubes of TIP3P [12] water molecules, and all atoms within 2.6 Å of any protein atom or crystallographic water molecule were deleted on a group-wise basis. This resulted in a protein solvated by 5417 and 5325 water molecules for the inactive and active models respectively. All calculations were performed with periodic boundary conditions. Bonds containing hydrogen were constrained to their equilibrium bond lengths using the SHAKE algorithm [13]. Energy minimization was achieved using a combined approach of 100 steps of steepest descent followed by 1000 steps of conjugate gradient. Each model was then subject to 10 ps of molecular dynamics simulations at 1000 K with a representative structure saved every 1 ps during the trajectory. The elevated temperature was for greater sampling of conformational space. The leapfrog Verlet algorithm was used for numerical integration of Newton's equations of motion at 0.001 ps intervals. The ten structures saved during each trajectory were energy minimized with 100 steps of steepest descent. The ILs in the resulting ten models of the inactive procaspase-3 and active procaspase-3 showed a main chain RMSD (root mean square deviation) of 0.308 Å and 0.244 Å respectively, demonstrating that at least within the radius of convergence given by our simulation conditions there is a single overall conformation of the IL in each case.

Comparison of the final model of inactive procaspase-3 with the procaspase-7 template using the brute force alignment in LSQMAN [14] resulted in an overall RMSD of 0.416 Å, demonstrating good agreement between the target structure and the model. Similarly, the RMSD between our model of the active procaspase-3(V266E) and the wild-type caspase-3 template is 0.226 Å, excluding the L2′ residues, which must differ in the two structures due to its connectivity to the rest of the IL in procaspase-3 and its positioning in the active site in the adjacent heterodimer in the mature caspase-3 dimer.

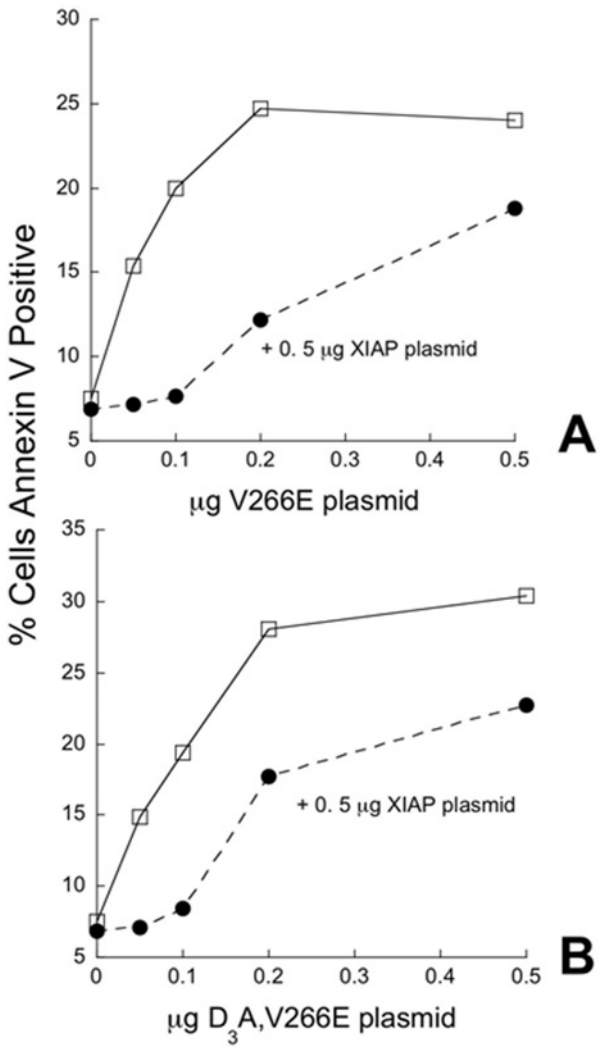

Figure S7 Poor inhibition of caspase-3 interface mutants by XIAP

(**A**) Co-transfection of caspase-3(V266E) with XIAP at various DNA ratios. (**B**) Co-transfection of caspase-3(D_3A,V266E) with XIAP at various DNA ratios. Transfections were performed with increasing amounts of caspase-3 vector in the presence of a constant amount of XIAP vector (●). The control in the absence of XIAP is shown as □. Cells were quantified by FACS for Annexin V staining 20 h post-transfection.

Table S1 Summary of data collection and refinement statistics for caspase-3(V266E)

Space group	I222			
Unit cell	a = 69.224 Å b = 84.607 Å c = 96.171 Å $\alpha = 90°$ $\beta = 90°$ $\gamma = 90°$			
Temperature (K)	100			
Resolution (Å)	1.63			
Number of reflections	41720			
Completeness (%)	99			
Redundancy	3.0			
R_{sym} (%)[a]	11.1			
Average I/σ	17.8 (6.1)			
R_{work} (%)[b]	20.17			
R_{free} (%)[c]	23.54			
RMSD for bond lengths (Å)	0.005			
RMSD for bond angles (Å)	1.2			
Number of protein atoms	1939			
Number of water molecules	297			
Ramachandran statistics				
	WT	V266E	Procaspase-3 (inactive)	Procaspase-3 (active)
In preferred regions	235 (96.7%)	233 (97.9%)	416 (88.1%)	452 (93.4%)
In allowed regions	5 (2.1%)	5 (2.1%)	47 (10%)	28 (5.8%)
Outliers	3 (1.2%)	0 (0%)	9 (1.9%)	4 (0.8%)

[a] $R_{sym} = \sum |Ii - < I > | / \sum I$

[b] $R_{work} = \sum ||F_0| - |F_c|| / \sum |F_0|$, calculated by using 90 % of the reflections against which the model was refined.

[c] $R = \sum ||F_0 - |F_c|| / \sum |F_0|$, calculated by using a test set consisting of 10 % of the total reflections, randomly selected from the original data set.

REFERENCES

1 Pop, C., Feeney, B., Tripathy, A. and Clark, A. C. (2003) Mutations in the procaspase-3 dimer interface affect the activity of the zymogen. Biochemistry **42**, 12311–12320

2 Stennicke, H. R., Jurgensmeier, J. M., Shin, H., Deveraux, Q., Wolf, B. B., Yang, X., Zhou, Q., Ellerby, M., Ellerby, L. M., Bredesen, D. et al. (1998) Pro-caspase-3 is a major physiologic target of caspase-8. J. Biol. Chem. **273**, 27084–27090

3 Janicke, R. U., Sprengart, M. L., Wati, M. R. and Porter, A. G. (1998) Caspase-3 is required for DNA fragmentation and morphological changes associated with apoptosis. J. Biol. Chem. **273**, 9357–9360

4 MacKenzie, S. H. and Clark, A. C. (2008) Targeting cell death in tumors by activating caspases. Curr. Cancer Drug Targets **8**, 98–109

4a Dechene, M., Wink, G., Smith, M., Swartz, P. and Mattos, C. (2009) Multiple solvent crystal structures of ribonuclease A: an assessment of the method. Proteins **76**, 861–881

5 Maly, D. J., Leonetti, F., Backes, B. J., Dauber, D. S., Harris, J. L., Craik, C. S. and Ellman, J. A. (2002) Expedient sold-phase synthesis of fluorogenic protease substrates using the 7-amino-4-carbamoylmethylcoumarin (ACC) fluorophore. J. Organic Chem. **67**, 910–915

6 Cullen, S. P., Luthi, A. U. and Martin, S. J. (2008) Analysis of apoptosis in cell-free systems. Methods **44**, 273–279

7 McStay, G. P., Salvesen, G. S. and Green, D. R. (2008) Overlapping cleavage motif selectivity of caspases: implications for analysis of apoptotic pathways. Cell Death Differ. **15**, 322–331

8 Brooks, B. R., Bruccoleri, R. E., Olafson, B. D., States, D. J., Swaminathan, S. and Karplus, M. (1983) CHARMM: A program for macromolecular energy, minimization, and dynamics calculations. J. Comp. Chem. **4**, 187–217

9 Arnold, K., Bordoli, L., Kopp, J. and Schwede, T. (2006) The SWISS-MODEL workspace: a web-based environment for protein structure homology modelling. Bioinformatics **22**, 195–201

10 Emsley, P. and Cowtan, K. (2004) COOT: model-building tools for molecular graphics. Acta Crystallogr. Sect. D Biol. Crystallogr. **60**, 2126–2132

11 Feeney, B., Pop, C., Swartz, P., Mattos, C. and Clark, A. C. (2006) Role of loop bundle hydrogen bonds in the maturation and activity of (pro)caspase-3. Biochemistry **45**, 13249–13263

12 Jorgensen, W. L., Chandrasekhar, J., Madura, J. D., Impey, R. W. and Klein, M. L. (1983) Comparison of simple potential functions for simulating liquid water. J. Chem. Phys. **79**, 926–935

13 Ryckaert, J. P., Ciccotti, G. and Berendsen, H. J. C. (1977) Numerical integration of the cartesian equations of motion of a system with constraints: molecular dynamics of n-alkanes. J. Comp. Phys. **23**, 327–341

14 Kleywegt, G. J. (1996) Use of non-crystallographic symmetry in protein structure refinement. Acta Crystallogr. Sect. D Biol. Crystallogr. **52**, 842–857

Received 29 May 2009/8 September 2009; accepted 30 September 2009
Published as BJ Immediate Publication 30 September 2009, doi:10.1042/BJ20090825